

## Will gradient crystals become available for neutron diffraction?

A. Magerl <sup>a,\*</sup>, K.-D. Liss <sup>a</sup>, C. Doll <sup>a</sup>, R. Madar <sup>b</sup>, E. Steichele <sup>c</sup>

<sup>a</sup> Institut Laue Langevin, F-38042 Grenoble Cedex, France

<sup>b</sup> INPG-ENSPG-LMGP Domaine Universitaire, F-38402 St. Martin-d'Hères, France

<sup>c</sup> Physik Department der TU München, E 21, D-85748 Garching, Germany

We report on a novel approach to grow massive  $\text{Si}_{1-x}\text{Ge}_x$  crystals by a low pressure chemical vapor deposition technique. In particular, we attempt to synthesize gradient crystals suited as monochromators in neutron- (and X-ray) scattering. Structural parameters for a large number of  $\text{Si}_{1-x}\text{Ge}_x$  deposits have been analysed by various techniques from materials science and representative examples are shown. Neutron diffraction profiles demonstrate the high quality of the crystals which could make them well suited for future applications.

### 1. Introduction

To date almost exclusively mosaic crystals are being used as neutron- and X-ray monochromators when intensity needs to be enhanced as compared to intensities available from perfect crystals. A typical gain factor in neutron scattering is  $G = 1000$ .

There has been a long standing interest in gradient crystals [1–5], i.e. single crystals with a smooth variation of the interplanar lattice spacing  $d$  along a defined crystallographic direction. They represent an alternative to mosaic crystals and allow similar or even higher intensity gains. The point in requesting both mosaic and gradient crystals is, that their diffracted phase space elements are distinctly different in shape, and, consequently, the performance of an instrument employing one or the other type of monochromator (or analyser) crystal will be largely different as well. Thus having both types of crystals available would provide an additional degree of freedom for engineering optimized resolution functions. This fact is being stressed in various contributions to this workshop [6].

Nevertheless, gradient crystals are not in general use today. The reason is that it has not been possible in the past to make these crystals with a sufficient quality. We have adopted a novel approach to grow massive  $\text{Si}_{1-x}\text{Ge}_x$  gradient crystals by a Low Pressure Chemical Vapor Deposition (LPCVD) technique. A first account on the experimental technique has been given else-

where [7,8]. In section 2 we will comment on various techniques on how to realize gradients in lattice spacings with emphasis on the binary alloy  $\text{Si}_{1-x}\text{Ge}_x$ . In section 3 we demonstrate the possibilities of growing  $\text{Si}_{1-x}\text{Ge}_x$  crystals from a materials science viewpoint by presenting a selection of experimental observations from this field. First results for the diffraction properties of various  $\text{Si}_{1-x}\text{Ge}_x$  crystals are shown in section 4, and in section 5 we comment on the perspectives of the availability of gradient crystals for beam definition.

### 2. How to make gradient crystals

B. Alefeld used a temperature difference  $\Delta T$  across a  $\text{CaF}_2$ -111 crystal in an early attempt to exploit the potential of gradient crystals [9]. He observed an intensity gain of  $G = 37$  for  $\Delta T = 230$  K with a very favourable shape of the diffraction profile characterized by steep edges. An increase of the reflectivity of  $G = 50$  was measured recently, when R. Hock et al. applied a longitudinal ultra sound wave to a perfect Si-111 crystal [10]. It should be noted that bending blades of perfect crystals also produces a gradient of the lattice spacing together with a variation of the inclination of the crystal planes along usual beam paths [11]. Even the increased reflectivity with  $G = 10$  related to precipitate structures in solids can be dominated by the longitudinal components of the strain field [12]. As a common disadvantage for all these techniques mentioned it appears, that an intensity gain by  $G = 1000$  seems at present out of reach.

\* Corresponding author. Present address: Ruhr-Universität Bochum, Festkörperphysik, D-44780 Bochum, Germany.

Single crystalline alloys with a continuously varying composition may be a promising alternative for gradient crystals. They could be brought about by a progressively increasing occupation of interstitial lattice sites along one dimension of the crystal as it occurs e.g. for critical fluctuations in some metal-hydrogen systems [13]. However long-time stability and a complex crystal environment could cause problems in applications. Substitutional alloys seem advantageous and the system  $\text{Si}_{1-x}\text{Ge}_x$  is a particularly favourable combination: both elements are well suited for thermal neutron (and for X-ray) scattering and they crystallize in the entire concentration range  $0 < x < 1$  in the cubic diamond structure [14]. The lattice constant of Ge exceeds the value of Si by 4.2%, from which a maximum gain factor of  $G = 2000$  is calculated for Si-111.

All attempts to pull massive single crystals of  $\text{Si}_{1-x}\text{Ge}_x$  alloys from the melt have failed so far for the following two main reasons: (i) the solidus and the liquidus lines in the phase diagram are widely separated and the melting points of Ge (1210 K) and of Si (1685 K) are not too different. This causes strong mass transport processes during crystal growth, and the solidification front becomes very unstable. (ii) although Si crystals are mechanically very strong at ambient temperature they become unusually soft above say 1300 K. Thus the presence of impurities like Ge atoms in a Si lattice will cause long-range defect structures, and a single crystal of high perfection cannot be grown any longer.

These problems are avoided in an epitaxial CVD growth process: the growth temperature can be low-

ered into a range where the Si lattice retains sufficient strength and the mixing of the components is readily performed in the gas phase. However, usual deposition rates are 0.1 to 1 Å/s. Then the time to grow a massive crystal of 1 cm thickness would be between 3 and 30 years! Thus our aim was to develop a very rapid epitaxy process with a growth rate of about 100 Å/s (1 mm/day = 116 Å/s), and which maintains a sufficient crystalline quality. The solution adopted is a high temperature LPCVD process based on silane and germane gases or their halogene derivatives. The layout of the apparatus is shown in Fig. 1 and more details can be found in ref. [7,8].

### 3. Properties of deposited $\text{Si}_{1-x}\text{Ge}_x$ crystals

Close to 100 crystals were grown on Si substrates during the last three years. Most samples had a surface of 5 cm<sup>2</sup> and the deposited layers were between 0.01 and 0.1 mm thick. They were mainly used to study and to optimize growth conditions and structural properties. In a few cases the thickness of the specimen reached about 1 mm. Also some experience has been gained by depositing on Si substrates with a diameter of 10 cm. Characteristic results for various aspects of the structural properties of layers, as they can now be deposited routinely, are presented in the following.

#### 3.1. Growth velocities

Very high growth velocities, while maintaining good crystalline quality of the deposited layer, is a key issue of our technique. This requires a high surface mobility of the adsorbed atoms, which becomes more pronounced at elevated deposition temperatures. These conditions also favour a complete decomposition of the Si- and Ge-carrying gases, and no further stimulation process like plasma enhancement or laser induction is needed. Growth rates have been determined consistently by a variety of techniques like the mass increase of the specimen, from RBS and from microprobe analysis, or by an inspection of the thickness of grown layers in an optical microscope. Fig. 2 gives typical growth rates for different silane flow rates and for various temperatures. The growth rate first increases with both silane throughput and temperature, until it levels off at a rate of about 1 mm/day ( $\cong 0.7 \mu\text{m}/\text{min}$ ) at a temperature of about 1300 K. This demonstrates the possibility to achieve the envisaged high growth rates in a temperature range where the Si-lattice is still rigid enough to incorporate the bigger Ge atoms as point defects. At 1300 K no further growth stimulating technique seems to be necessary because the decomposition of silane and germane into their chemical elements is already complete.

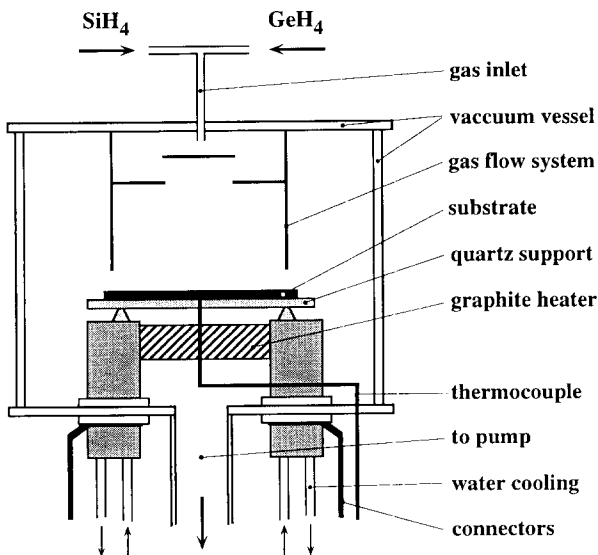


Fig. 1. Layout of the LPCVD reactor.

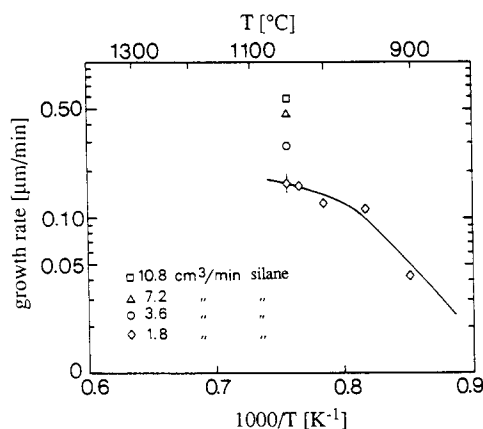


Fig. 2. Growth rates for various silane through-puts (solid line is drawn as a guide to the eye).

### 3.2. Growth morphology

The structural properties of the deposits depend strongly on the growth conditions. In general higher growth rates also require higher substrate temperatures to maintain good single crystalline quality. This can be readily appreciated from the morphology of the surface. Fig. 3 gives an illustrative example for three specimen made at high rates of about 0.5 mm/day. At low temperature (1200 K) only an amorphous deposit with a rough, cauliflower-like surface is observed. Epitaxial growth sets in at intermediate temperatures (1300 K), where defects on the surface show very nicely the crystallographic symmetry of the substrate (e.g. a Si-111 wafers were used for the samples in Fig. 3). At even higher temperature (1450 K) the growth morphology changes again. A step growth process becomes dominant as evidenced by the appearance of a pronounced terrace structure [15]. It seems that the intermediate temperature range is best suited for our purpose, because the conditions for mechanical stability, high growth rate and single crystalline quality are fulfilled simultaneously.

### 3.3. Microprobe analysis

The Si–Ge composition profile can be analysed quantitatively with a lateral spatial resolution of about 2 μm by electron micro probe analysis. Fracture planes perpendicular to the growth direction provide access to the entire epitaxial layer. Fig. 4a shows the Ge profile for a sample with two fixed concentrations of  $x = 0.032$  and  $x = 0.068$ . The thickness for each layer is about 30 μm. The profile of the steps corresponds to the instrumental resolution. This demonstrates that interdiffusion of Si and Ge is insignificant for our growth condi-

tions. These data is also very valuable to correlate the composition of the solid with the mixing ratio of the gases and to access the change of the growth rate with composition. This will be fully presented in a forthcoming paper. Fig. 4b shows the concentration profile of a  $\text{Si}_{1-x}\text{Ge}_x$  gradient crystal with a linear increase of  $x$  up to a maximum Ge value similar as the one in Fig. 4a. First a 10 μm thick layer supposedly free of Ge was grown. This part corresponds to the range  $-10 < t < 0$  μm in Fig. 4b. However, this layer contains already  $x = 0.001$  Ge due to a leakage in our gas handling system. This leak also perturbs the composition of the next 10 μm. However, it becomes insignificant for higher values of the Ge concentration, and a good linear dependence up to the maximum thickness of the crystal at about 80 μm is found.

The highest Ge concentrations synthesized so far correspond to  $x = 0.4$ . This value is imposed by the present layout of the gas handling system. So far no other limitations have shown up.

### 3.4. Rutherford backscattering (RBS)

RBS is another highly valuable tool to access structural properties of deposited layers. It is very advantageous for stepped concentration profiles and for thin epitaxial structures limited to about 10 μm. In contrast to microprobe analysis the sample is analysed over a large surface area in the cm<sup>2</sup> range. Fig. 5 gives a typical example of a RBS spectrum taken with 1.4 MeV protons [16]. Starting from high energy, the Ge edge, the Si edge, and a negative Ge edge is clearly distinguished. A quantitative evaluation reveals an 11 μm thick Ge layer with  $x = 0.03$  on a pure Si substrate.

In addition, the channeling effect in RBS can be exploited to yield information on the single crystalline quality of the layers averaged over a large area. Ions impinging at an arbitrary direction onto the surface of the sample experience a high backscattering yield. If the trajectory of the ion lines up with a high symmetry direction in a single crystal of good quality, then the ion may penetrate deep into the bulk of the material, and the fraction of backscattered ions (at a given energy) drops significantly. Fig. 6 shows the channeling of He atoms along the [100] growth direction in an epitaxially grown  $\text{Si}_{1-x}\text{Ge}_x$  crystal with  $x = 0.06$ . The most important parameter is the amplitude of the reduction of the backscattering yield, which amounts to  $K' = 0.90$  in Fig. 6. For comparison, a perfect Si crystal would show  $K_0 = 0.97$  under the same experimental conditions. The deliberate introduction of Ge point defects into the Si lattice causes some waviness of the atomic planes, which likely accounts for the major part of the difference between  $K_0$  and  $K'$  [16]. The channeling data in Fig. 6 definitely emphasize a high crystalline fidelity of the deposited  $\text{Si}_{1-x}\text{Ge}_x$  crystal.

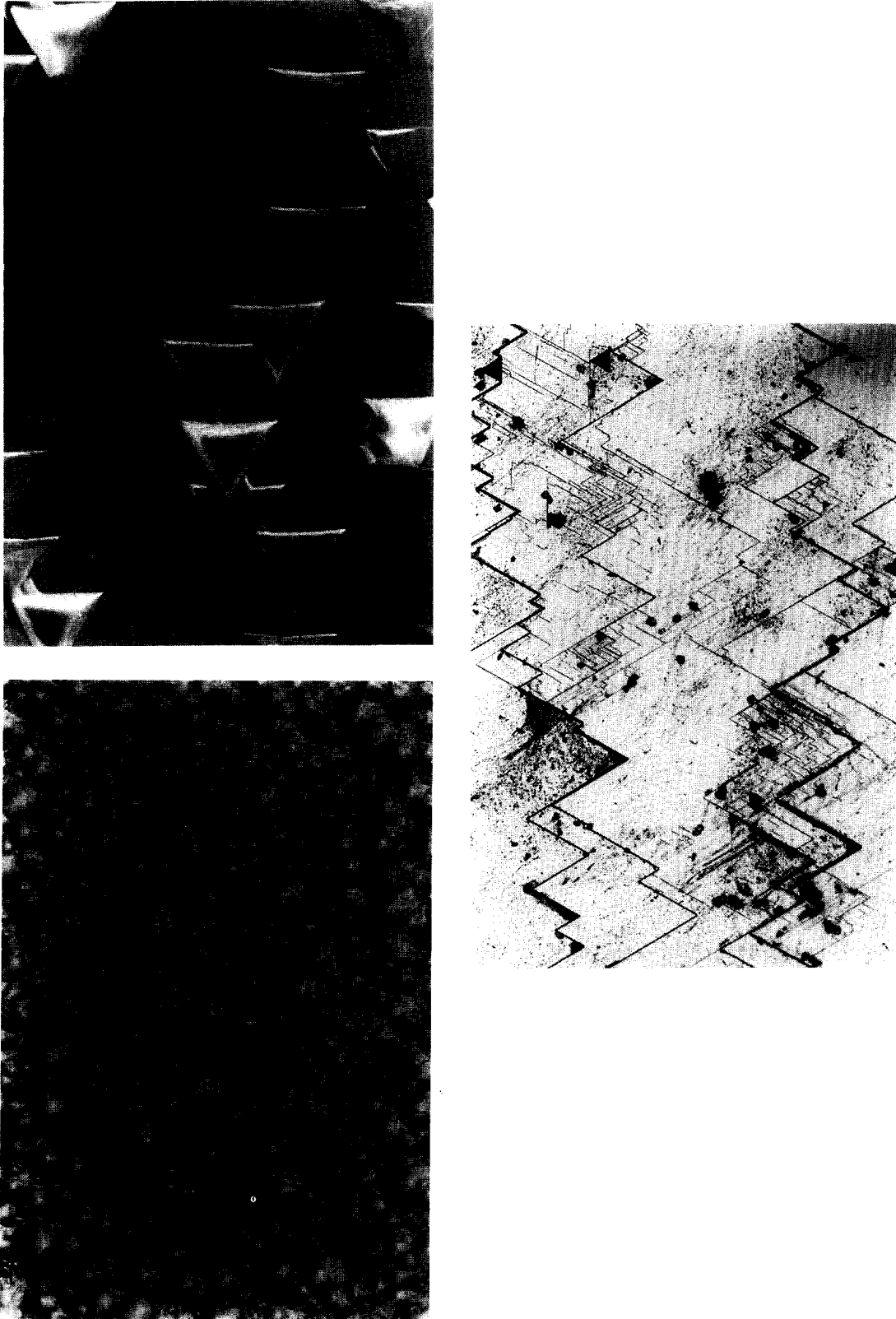


Fig. 3. Surface aspects of deposited layers on a Si-111 substrate at high deposition rates (about 0.5 mm./day) at 1100 K (top left), 1300 K (top right) and 1450 K (bottom). The width of the figures corresponds to about 0.1 mm.

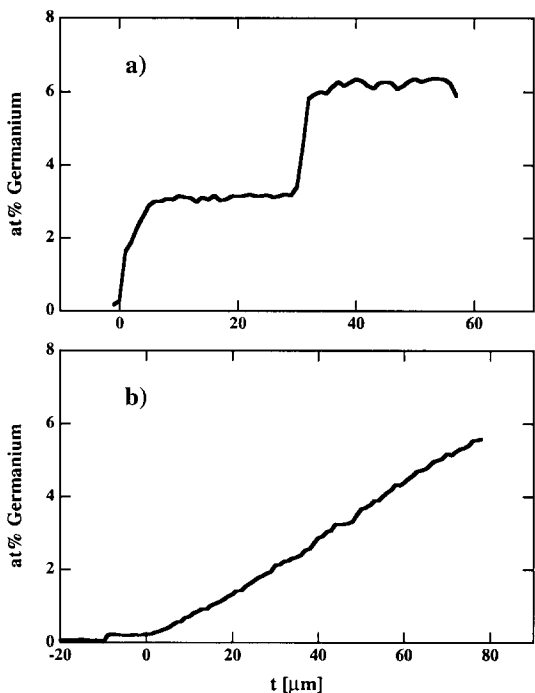


Fig. 4. Ge concentration profile from micro probe analysis for a  $\text{Si}_{1-x}\text{Ge}_x$  crystal with a stepped (a) and a continuous (b) variation of the composition.

#### 4. Neutron diffraction

The most crucial test for the real value of the synthesized  $\text{Si}_{1-x}\text{Ge}_x$  crystals concerns their neutron reflectivity, which is illustrated in this chapter. All reflectivity data presented here have been taken at very high Bragg angles in a backscattering or near backscattering setup. (Bragg angle  $\theta \geq 89^\circ$ ). Under these conditions the mosaicity of the sample and the divergence of the beam are not of relevance, and the spectra reflect directly the distribution of the lattice spacing  $d$ . Furthermore, all data shown are based on Si-111 reflections.

As a reference Fig. 7a shows the transmission curve for a perfect Si-111 sample measured in a double crystal setup [17]. The observed dip in the spectrum represents the – small – reflecting power of a perfect monochromator. The width of the dip appears broader by a factor of 2.5 than its extinction-limited value. Consequently, its depth is not fully developed. However, the integrated reflectivity agrees well with the theoretical prediction [17–20].

Fig. 7 shows the transmission spectrum of a  $\text{Si}_{1-x}\text{Ge}_x$  crystal measured in a similar setup [15]. The concentration  $x$  has been kept fixed, and the Si substrate has been removed mechanically. The transmission dip is found shifted by  $\Delta d/d = -3.1 \times 10^{-3}$  from

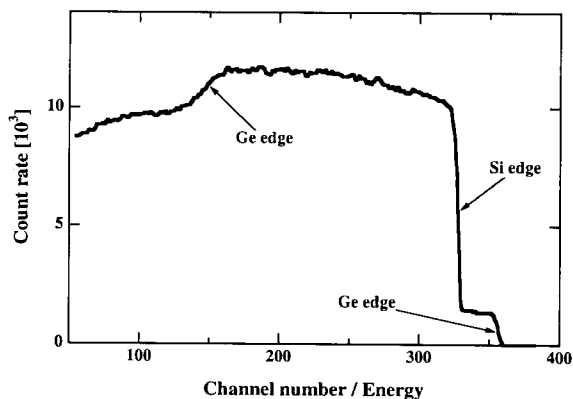


Fig. 5. RBS spectrum of 1.4 MeV protons. The data show a 11  $\mu\text{m}$  thick  $\text{Si}_{1-x}\text{Ge}_x$  layer with  $x = 0.03$  on a pure Si substrate.

the zero position, which corresponds to  $x = 0.089$ . It is important to note, that the width of the dip has only increased slightly compared to ideal Si in Fig. 7a, indicating that a very homogeneous crystal of high structural quality has been grown.

This particular composition of  $x = 0.089$  is very interesting for a monochromator on cold neutron backscattering spectrometers like IN10 at the ILL [21]. Usually perfect Si crystals are used as monochromator and analyser on this spectrometer of highest energy resolution. The energy is scanned using the Doppler effect from a rapid mechanical motion of the monochromator, which limits the scan range to  $\pm 15 \mu\text{eV}$  with an instrumental resolution of about  $1 \mu\text{eV}$ . Replacing the Si monochromator by a  $\text{Si}_{1-x}\text{Ge}_x$  monochromator with  $x = 0.089$  offsets the scan range by  $-13 \mu\text{eV}$ . The scan range of the instrument now extends from  $-28 \mu\text{eV}$  to  $2 \mu\text{eV}$ . Thus the dynamical range accessible on this type of spectrometer effectively has been doubled without a significant loss in resolution. Other offsets close to  $-200 \mu\text{eV}$  can be created by choosing appropriate Ge concentrations.

A  $\text{Si}_{1-x}\text{Ge}_x$  monochromator with  $x = 0.089$  has been assembled out of several individual crystals. It is routinely available on IN10 and first measurements have been reported by A. Magerl and C. Holm [15].

A crystal with six concentration steps reaching up to a maximum value of  $x = 0.32$  has been made in order to exploit further the potential over this extended range. All layers were grown for the same deposition time. This large sample with a surface of  $20 \text{ cm}^2$  has been tested on the high resolution time-of-flight diffractometer at the research reactor FRM at Munich. A spectrum measured in reflection geometry is presented in Fig. 7c. A first strong and narrow reflection peak is observed at  $\Delta d/d = 0$ . It originates from the pure Si substrate. Further reflections are located at  $\Delta d/d[\%] = 0.34, 0.58, 0.81, 1.02, 1.20,$  and  $1.35$  corresponding to deposited  $\text{Si}_{1-x}\text{Ge}_x$  layers with  $x = 0.08,$

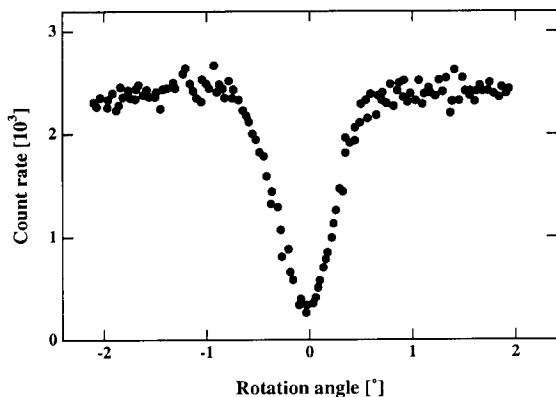


Fig. 6. Channeling of He atoms in a  $\text{Si}_{1-x}\text{Ge}_x$  crystal with  $x = 0.06$ . Rotation angle 0 corresponds to channeling along the [100] growth direction.

0.14, 0.19, 0.24, 0.29 and 0.32, respectively. Their peak intensities are significantly lower and their widths are much larger than the substrate peak. Furthermore, the integrated intensity of these peaks seems to diminish with increasing concentration. The experimental results are also summarized in Table 1.

The values for the thickness of the individual layers have been determined by micro probe analysis and they are also given in Table 1. It can be noted, that the thicknesses become less with increasing  $x$  values indicating a reduction of the growth velocity at higher Ge concentrations. The principal features concerning the peak intensities and the peak shapes can be explained by the fact that the deposited layers are thinner than the extinction length which is  $37 \mu\text{m}$  for perfect Si-111. The experimental results are also summarized in Table 1. As the salient feature from Fig. 7c we note that single crystalline layers have been deposited on a Si-111 substrate at several concentrations reaching up to  $x = 0.32$ , which corresponds to  $\Delta d/d = 1.3\%$ . The quality of the layers is sufficient to give well defined Bragg peaks for the entire concentration range explored so far.

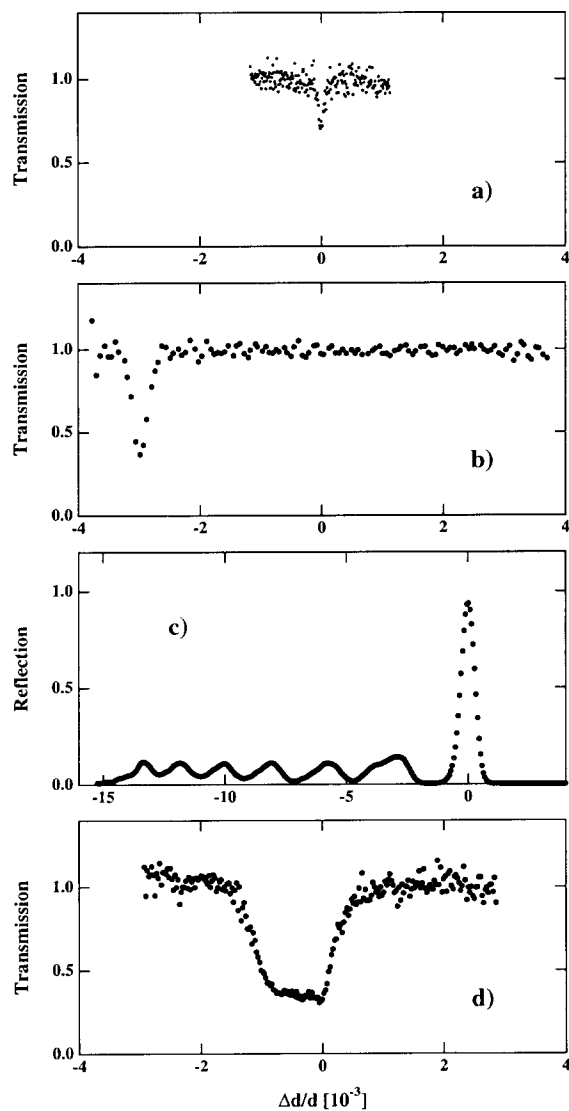


Fig. 7. Neutron reflectivity data measured on various  $\text{Si}_{1-x}\text{Ge}_x$  crystals at very high Bragg angles in transmission (a, b, d) or reflection geometry (c). See text for details. Note the different scales for the abscissae.

Table 1

Geometrical parameters and reflectivity values for a six-step  $\text{Si}_{1-x}\text{Ge}_x$  crystal. Peak widths and integrated intensities are normalized to the values for the pure Si substrate. (The thickness for layer number 6 may be somewhat uncertain due to a possible slight damage of the top layer during mechanical preparation for micro probe analysis)

Layer number	1	2	3	4	5	6
Layer thickness [ $\mu\text{m}$ ]	19	14	8	7	6	(4–5)
Concentration [ $x$ ]	0.08	0.14	0.19	0.24	0.29	0.32
$\Delta d/d$ [%]	0.34	0.58	0.81	1.02	1.20	1.35
Integrated peak intensity	0.57	0.17	0.15	0.11	0.10	0.07

For a gradient crystal the concentration  $x$  needs to be varied continuously during crystal growth. Actually, one would expect an improved crystalline quality for a gradient crystal with a smooth variation of the lattice spacing as compared to a crystal with a stepped concentration profile, and first experimental evidence from high energy X-ray diffraction supports this assumption [22].

In a 24 hour experiment a crystal with a linear concentration profile of  $0 < x < 0.035$  and with a thickness of 0.8 mm has been grown. This corresponds to a theoretical variation of the lattice spacing of  $\Delta d/d = 1.5 \times 10^{-3}$  with a peak reflectivity of 0.75. (An ideal gradient crystal with a peak reflectivity close to 1 could be envisaged as well. It would require a 2 to 3 times lower gradient, i.e. 2 to 3 times thicker crystal for the same  $\Delta d/d$  value). The transmission spectrum for this crystal is shown in Fig. 7d. The integrated intensity exceeds the value for ideal Si by a factor of 70. Moreover, we note the particular lineshape characterized by steep edges and an almost horizontal plateau. Both the width and the amplitude of the transmission curve agree remarkably well with the expected values. This emphasizes the fact that the gradient crystal produced has an appropriate microstructure which can be very well controlled by a LPCVD production process.

## 5. Summary

Gradient crystals and mosaic crystals can be considered as complementary optical components for beam definition in neutron and X-ray scattering. However, gradient crystals are hardly used on spectrometers because it has not been possible to make them with a sufficiently good quality. In a novel approach we have tried to grow massive  $\text{Si}_{1-x}\text{Ge}_x$  crystals by a very fast LPCVD method. Neutron diffraction profiles presented demonstrate that it is possible to deposit high quality single crystalline alloys with either fixed or gradually changing Ge concentration. The highest concentrations reached is  $x = 0.4$ , this value being limited only by the layout of our gas handling system. For the gradient crystals produced so far, we could demonstrate that the peak profile and the reflectivity measured correspond well with the expected performance.

Most of the samples made were based on Si substrates with a surface of  $4 \text{ cm}^2$ . We are engaged in a program to increase the substrate size up to 10 cm diameter wafers and we consider for the future an extension such that deposits can be made either on Si- or Ge-substrates.

## Acknowledgement

We appreciate the stimulating interest of T. Springer, KFA Jülich, in this project and we want to thank A. Escoffier for his enthusiastic help on the crystal growth reactor.

## References

- [1] H. Maier-Leibnitz and F. Rustichelli, patent number 1816542, Deutsches Patentamt, submitted 23-12-1968.
- [2] F. Rustichelli, Nucl. Instr. and Meth. 124 (1970) 83.
- [3] F. Rustichelli, Proc. Int. Conf. on Neutron Inelastic Scattering 1972, IAEA-SM-155/F2 (International Atomic Energy Agency, Vienna, 1972) p. 697.
- [4] A. Freund, P. Guinet, J. Mareschal, F. Rustichelli and F. Vanoni, J. Crystal Growth 13&14 (1972) 726.
- [5] A. Boeuf, P. Detourbet, A. Escoffier, R. Hustache, S. Lagomarsino, A. Rennert and F. Rustichelli, Nucl. Instr. and Meth. 152 (1978) 415.
- [6] R. Scherm and E. Krüger, these Proceedings (Workshop on Focusing Bragg Optics, Braunschweig, Germany, 1993), Nucl. Instr. and Meth. A 338 (1994) 1; B. Dorner, op. cit. p. 32; K.-D. Liss and A. Magerl, op. cit. p. 90.
- [7] R. Madar, E. Mastromatteo, A. Magerl and K.-D. Liss, Surface and Coatings Technology 54&55 (1992) 229.
- [8] A. Escoffier, R. Madar, A. Magerl and E. Mastromatteo, French patent number 91/09109.
- [9] B. Alefeld, Z. Physik 228 (1969) 454.
- [10] R. Hock, T. Vogt, J. Kulda, Z. Mursic, H. Fuess and A. Magerl, Z. Physik B: Condensed Matter 90 (1993) 143.
- [11] See e.g. P. Mikula, these Proceedings (Workshop on Focusing Bragg Optics, Braunschweig, Germany, 1993), Nucl. Instr. and Meth. A 338 (1994) 17.
- [12] A. Magerl, J.R. Schneider and W. Zulehner, J. Appl. Phys. 67 (1990) 533.
- [13] H. Zabel and H. Peisl, Acta Metallurgica 28 (1980) 589.
- [14] M. Hansen, Constitution of Binary Alloys (McGraw-Hill, New York, 1958).
- [15] This sample has been grown by a modified CVD technique described in: A. Magerl and C. Holm, Nucl. Instr. and Meth. A 290 (1990) 414.
- [16] A. Magerl, L. Ligeon, B. Daudin and M. Dubus, to be published.
- [17] M. Birr, A. Heidemann and B. Alefeld, Nucl. Instr. and Meth. 95 (1971) 435.
- [18] C.G. Darwin, Phil. Mag. 27 (1914) 315.
- [19] P.P. Ewald, Ann. Physik 54 (1917) 519.
- [20] H. Rauch and D. Petrascheck, Grundlagen für ein Laue-Neutroneninterferometer – Teil 1 Dynamische Beugung, AIAU 74405b, Vienna (1976).
- [21] See: Neutron Research Facilities at the ILL High Flux Reactor, ed. B. Maier, Institut Laue–Langevin, Grenoble (1983).
- [22] A. Magerl et al., to be published.